

# RIFE: Real-Time Intermediate Flow Estimation for Video Frame Interpolation

Zhewei Huang<sup>1</sup> Tianyuan Zhang<sup>1</sup> Wen Heng<sup>1</sup> Boxin Shi<sup>2</sup> Shuchang Zhou<sup>1</sup>

<sup>1</sup>Megvii Inc <sup>2</sup>Peking University

{huangzhewei, zhangtianyuan, hengwen, zsc}@megvii.com, shiboxin@pku.edu.cn

## Abstract

We propose RIFE, a Real-time Intermediate Flow Estimation algorithm for Video Frame Interpolation (VFI). Many recent flow-based VFI methods first estimate the bi-directional optical flows, then scale and reverse them to approximate intermediate flows, leading to artifacts on motion boundaries. RIFE uses a neural network named IFNet that can directly estimate the intermediate flows from coarse-to-fine with much better speed. We design a privileged distillation scheme for training intermediate flow model, which leads to a large performance improvement. Experiments demonstrate that RIFE is flexible and can achieve state-of-the-art performance on several public benchmarks. The code is available at <https://github.com/hzwer/arXiv2020-RIFE>

## Introduction

Video Frame Interpolation (VFI) aims to synthesize intermediate frames between two consecutive video frames. It is widely used to improve frame rate and enhance visual quality. Moreover, real-time VFI algorithms running on high-resolution videos have many potential applications, such as increasing the frame rate of video games and live videos and providing video enhancement services for users with limited computing resources.

VFI is challenging due to the complex, large non-linear motions and illumination changes in the real world. Recently, flow-based VFI algorithms have offered a framework to address these challenges and achieved impressive results (Liu et al. 2017; Jiang et al. 2018; Niklaus and Liu 2018; Xue et al. 2019; Bao et al. 2019; Xu et al. 2019; Liu et al. 2020). Common approaches for these methods involve two steps: 1) warping the input frames according to approximated optical flows and 2) fusing and refining the warped frames using Convolutional Neural Networks (CNNs).

Given the input frames  $I_0, I_1$ , flow-based methods (Liu et al. 2017; Jiang et al. 2018; Bao et al. 2019) need to approximate the intermediate flows  $F_{t \rightarrow 0}, F_{t \rightarrow 1}$  from the perspective of the frame  $I_t$  that we are expected to synthesize. There is a “chicken-and-egg” problem between intermediate flows and frame because  $I_t$  is not available during the inference phase and its estimation is a difficult problem (Jiang et al. 2018; Park et al. 2020). Many practices (Jiang et al. 2018; Bao et al. 2019; Xu et al. 2019; Liu et al. 2020) first compute bi-directional flows from state-of-the-art optical flow mod-

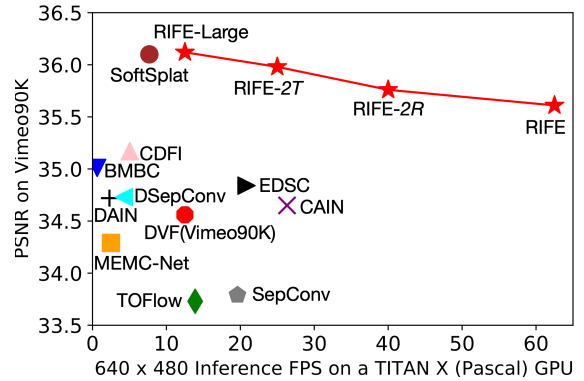


Figure 1: **Speed and accuracy trade-off by adjusting model size setting.** We compare our RIFE with previous VFI methods on Vimeo90K benchmark (Xue et al. 2019).

els, then reverse and refine them to generate intermediate flows. However, they may have flaws in motion boundaries, as the object position changes from frame to frame. Another pioneering work, DVF (Liu et al. 2017) proposes voxel flow to jointly model the intermediate flow and occlusion mask and uses CNNs to estimate them end-to-end. AdaCoF (Lee et al. 2020a) further extends intermediate flow to adaptive collaboration of flows. BMBC (Park et al. 2020) designs a bilateral cost volume operator to obtain more accurate intermediate flows.

Despite the improvement of image quality, the frame interpolation model is becoming more and more complex. It is desired to explore the conciseness of directly intermediate flow estimation such as DVF (Liu et al. 2017) while maintaining state-of-the-art performance. But this is challenging for existing flow-based VFI models due to the following two issues:

- 1) Requiring some additional components: Image depth model (Bao et al. 2019), flow refinement model (Jiang et al. 2018) and flow reversal layer (Xu et al. 2019) are introduced to compensate for the defects of intermediate flow estimation. These methods also require pre-trained state-of-the-art optical flow models as substructures that are not specially designed for VFI tasks.
- 2) Lacking direct supervision for the approximated interme-

mediate flows: To the best of our knowledge, most previous interpolation models are trained with only the final reconstruction loss. There is no other supervision explicitly designed for the flow estimation process, degrading the performance of interpolation.

To address these issues, we propose IFNet adopting a coarse-to-fine strategy (Ilg et al. 2017) with progressively increased resolutions: it iteratively updates intermediate flows and soft fusion mask via successive IFBlocks. Conceptually, according to the iteratively updated flow fields, we could move corresponding pixels from two input frames to the same location in a latent intermediate frame and use a fusion mask to combine pixels from two input frames. Unlike most previous optical flow models (Dosovitskiy et al. 2015; Ilg et al. 2017; Sun et al. 2018; Hui, Tang, and Change Loy 2018; Teed and Deng 2020), IFBlocks do not contain expensive operators like cost volume or forward warping and use  $3 \times 3$  convolution and deconvolution as building blocks. IFNet is easier to deploy on some mobile devices because of its low computational cost and simple operator set.

We also argue that employing intermediate supervision is very important. When training the IFNet end-to-end with a later fusion process using the final reconstruction loss, our method produces worse results than previous methods that use complex pipelines and pre-trained flow models. The picture dramatically changes after we design a privileged distillation scheme that employs a teacher model with access to the intermediate frames to guide the student to learn.

Combining these designs, we propose the Real-time Intermediate Flow Estimation (**RIFE**). RIFE can achieve satisfactory results when trained from scratch. Our training does not require pre-trained optical flow models or datasets with optical flow labels. We illustrate the speed and accuracy trade-off compared with other methods in Figure 1.

In summary, our contributions are three-fold:

- We design an efficient coarse-to-fine IFNet using simple operators to directly approximate the intermediate flows given two input frames.
- We introduce a privileged distillation scheme for training the intermediate flow model, which leads to large performance improvement.
- We use model scaling and test-time augmentation to obtain models with varying quality and speed trade-offs to show RIFE’s flexibility. Our experiments show RIFE achieves state-of-the-art performance on several public benchmarks.

## Related Works

**Optical flow estimation** Optical flow estimation is a long-standing vision task that aims to estimate the per-pixel motion, which is useful in lots of downstream tasks. Since the milestone work of FlowNet (Dosovitskiy et al. 2015) based on U-net autoencoder (Ronneberger, Fischer, and Brox 2015), architectures for optical flow models have evolved for several years, yielding more accurate results while being more efficient, such as FlowNet2 (Ilg et al. 2017), PWC-Net (Sun et al. 2018) and LiteFlowNet (Hui, Tang, and

Change Loy 2018). Recently Teed *et al.* (Teed and Deng 2020) introduce RAFT, which iteratively updates a flow field through a recurrent unit and achieves a remarkable breakthrough in this field. Another important research direction is unsupervised optical flow estimation (Meister, Hur, and Roth 2018; Jonschkowski et al. 2020; Luo et al. 2021) due to the difficulty of optical flow labeling.

**Video frame interpolation.** VFI supports various applications like slow-motion generation, video compression (Wu, Singhal, and Krahenbuhl 2018), and novel view synthesis. Recently, optical flow a very popular approach to video interpolation. In addition to the method of directly estimating the intermediate flow (Liu et al. 2017; Lee et al. 2020a; Park et al. 2020), Jiang *et al.* (Jiang et al. 2018) propose SuperSlomo using the linear combination of the two bi-directional flows as an initial approximation of the intermediate flows and then refine them using U-Net. Reda *et al.* (Reda et al. 2019) propose to synthesize intermediate frames using unsupervised cycle consistency based on SuperSlomo. Bao *et al.* (Bao et al. 2019) propose DAIN to estimate the intermediate flow as a weighted combination of bidirectional flow. Niklaus *et al.* (Niklaus and Liu 2020) propose SoftSplat to forward-warp frames and their feature map using softmax splatting. Xu *et al.* (Xu et al. 2019) propose QVI to exploit four consecutive frames and flow reversal filter to get the intermediate flows. Liu *et al.* (Liu et al. 2020) further extends QVI with rectified quadratic flow prediction to EQVI.

Along with flow-based methods, flow-free methods have also achieved remarkable progress in recent years. Meyer *et al.* (Meyer et al. 2015) utilize phase information to learn the motion relationship for multiple video frame interpolation. Niklaus *et al.* (Niklaus, Mai, and Liu 2017a,b) formulate VFI as a spatially adaptive convolution whose convolution kernel is generated using a CNN given the input frames. Cheng *et al.* propose DSepConv (Cheng and Chen 2020b) to extend kernel-based method using deformable separable convolution and further propose EDSC (Cheng and Chen 2020a) to perform multiple interpolation. Choi *et al.* (Choi et al. 2020) propose an efficient flow-free method named CAIN, which employs the PixelShuffle operator and channel attention to capture the motion information implicitly.

**Privileged knowledge distillation.** Our privileged distillation (Lopez-Paz et al. 2015) for intermediate flow conceptually belongs to the knowledge distillation (Hinton, Vinyals, and Dean 2015) method, which originally aims to transfer knowledge from a large model to a smaller one. In privileged distillation, the teacher model gets more input than the student model, such as scene depth, images from other camera views, and even image annotation. Therefore, the teacher model can provide more accurate representations to guide the student model to learn. This idea is applied to some computer vision tasks, such as image super resolution (Lee et al. 2020b), hand pose estimation (Yuan, Stenger, and Kim 2019), re-identification (Porrello, Bergamini, and Calderara 2020) and video style transfer (Chen et al. 2020). Our work is also related to codistillation (Anil et al. 2018) where student and teacher have the same architecture and use distillation during training.

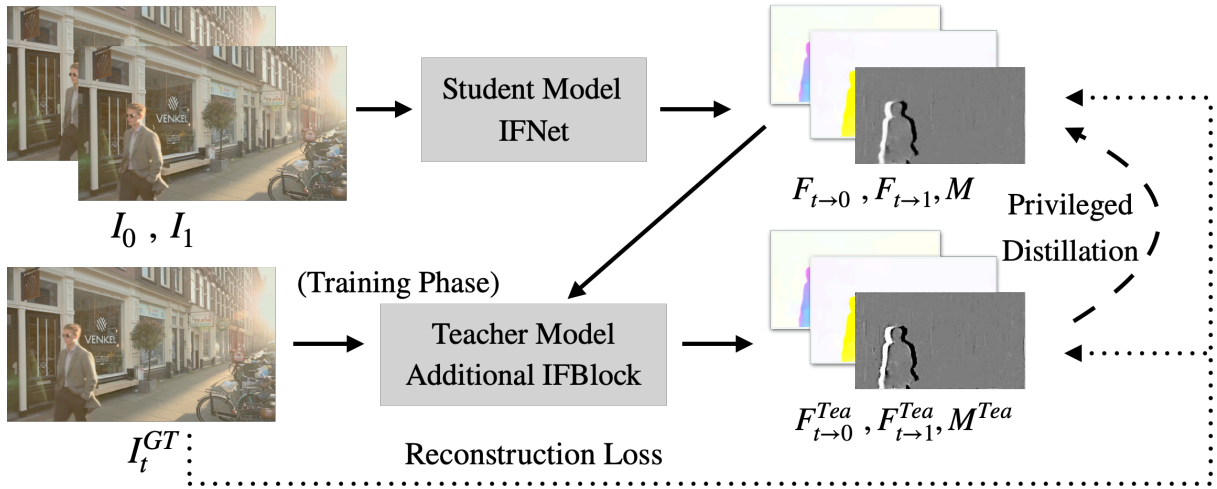


Figure 2: **Overview of RIFE training.** Given two input frames  $I_0, I_1$ , we directly feed them into our IFNet to approximate intermediate flows  $F_{t \rightarrow 0}, F_{t \rightarrow 1}$  and the fusion map  $M$ . During training phase, a privileged teacher refines student’s results to get  $F_{t \rightarrow 0}^{Tea}, F_{t \rightarrow 1}^{Tea}$  and  $M^{Tea}$  based on ground truth  $I_t$ . The student model and the teacher model are jointly trained from scratch using the reconstruction loss. The teacher’s approximations are more accurate so that they can guide the student to learn.

## Method

We first provide an overview of RIFE. Then we describe the efficient design of the major components in RIFE, elaborate on our proposed distillation scheme, and explain the training details.

### Pipeline Overview

We illustrate the overview of our proposed RIFE in Figure 2. Given a pair of consecutive RGB frames,  $I_0, I_1$ , our goal is to synthesize an intermediate frame  $\hat{I}_t$ , where  $t = 0.5$  is a common practice. We estimate the intermediate flows  $F_{t \rightarrow 0}, F_{t \rightarrow 1}$  and fusion map  $M$  by feeding input frames into IFNet. We can get reconstructed image  $\hat{I}_t$  using following formulation:

$$\hat{I}_t = M \odot \hat{I}_{t \leftarrow 0} + (1 - M) \odot \hat{I}_{t \leftarrow 1}, \quad (1)$$

$$\hat{I}_{t \leftarrow 0} = w(I_0, F_{t \rightarrow 0}), \hat{I}_{t \leftarrow 1} = w(I_1, F_{t \rightarrow 1}). \quad (2)$$

where  $w$  is the image backward warping,  $\odot$  is an element-wise multiplier, and  $(0 \leq M \leq 1)$ . We use another encoder-decoder CNNs named RefineNet following previous methods (Jiang et al. 2018; Niklaus and Liu 2020) to refine the high-frequency area of  $\hat{I}_t$  and reduce artifacts of the student model. Its computational cost is similar to IFNet, and the detailed architecture of RefineNet is in Appendix.

### Intermediate flow estimation

Some previous intermediate flow estimation methods reverse and refine bi-directional flows (Jiang et al. 2018; Xu et al. 2019; Bao et al. 2019; Liu et al. 2020) as depicted in Figure 3. The role of our IFNet is to directly and efficiently predict  $F_{t \rightarrow 0}, F_{t \rightarrow 1}$  and fusion mask  $M$  given two consecutive input frames  $I_0, I_1$ .

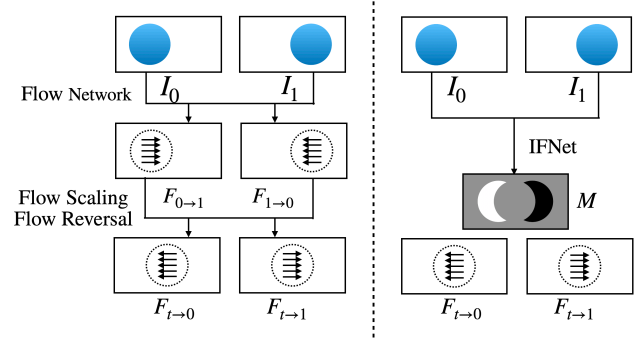


Figure 3: **Comparison between previous intermediate estimation approaches (Jiang et al. 2018; Xu et al. 2019; Bao et al. 2019; Liu et al. 2020) (left) and IFNet (right).** Recently VFI methods contain two stages: 1) bi-direction flow estimation and 2) flow reversal modules. The flow reversal process is usually cumbersome due to the difficulty of handling the changes of object positions. IFNet can directly estimate the intermediate flows.

To handle the large motion encountered in intermediate flow estimation, we employ a coarse-to-fine strategy with gradually increasing resolutions, as illustrated in Figure 4. Specifically, we first compute a rough prediction of the flow on low resolutions, which is believed to capture large motions easier, then iteratively refine the flow fields with gradually increasing resolutions. Following this design, our IFNet has a stacked hourglass structure, where a flow field is iteratively refined via successive IFBlocks:

$$(F^i, M^i) = (F^{i-1}, M^i) + g^i(F^{i-1}, M^{i-1}, \hat{I}^{i-1}), \quad (3)$$

where  $F^{i-1}, M^{i-1}$  denotes the current estimation of the intermediate flows and fusion map from the  $i - 1$ -th IFBlock,

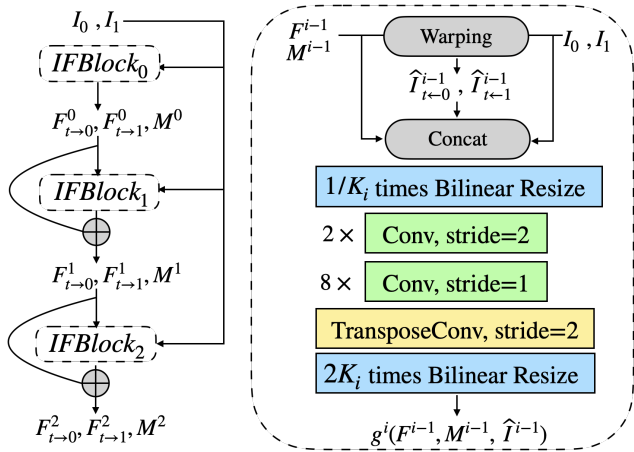


Figure 4: **Structure of IFNet.** **Left:** IFNet is composed of three stacked IFBlocks operating at different resolutions. **Right:** We first backwarp the two input frames based on current approximated flow  $F^{i-1}$ . Then the input frames  $I_0, I_1$ , warped frames  $\hat{I}_{t-0}^{i-1}, \hat{I}_{t-1}^{i-1}$  and the previous results  $F^{i-1}, M^{i-1}$  are fed into the next IFBlock to approximate flow and mask residuals.

Table 1: **Inference time on 720p video.** Recently flow-based VFI methods (Jiang et al. 2018; Bao et al. 2019; Niklaus and Liu 2020) run the optical flow model twice to obtain bi-directional optical flows.

Method	FlowNet2	PWC-Net	RAFT	IFNet
Runtime	$2 \times 207\text{ms}$	$2 \times 52\text{ms}$	$2 \times 145\text{ms}$	<b>17ms</b>

and  $g^i$  represents the  $i$ th IFBlock. We use a total of 3 IFBlocks, and each has a resolution parameter,  $K_i$ . To keep our design simple, each IFBlock has a feed-forward structure consisting of several convolutional layers and an up-sampling operator. Except for the layer that outputs the optical flow residuals and the fusion map, we use PReLU (He et al. 2015) as the activation function.

We compare the runtime of the current state-of-the-art optical flow models (Ilg et al. 2017; Sun et al. 2018; Teed and Deng 2020) and our IFNet in Table 1. Current flow-based methods (Jiang et al. 2018; Bao et al. 2019; Niklaus and Liu 2020) usually need to run their flow model twice to get the bi-directional flows then scale and reverse the flows. Therefore the intermediate flow estimation in RIFE runs at a faster speed than previous methods, achieving the acceleration of about 6 – 20 times. Although these optical models can estimate inter-frame motion accurately, they are not suitable for direct migration to VFI tasks.

### Privileged Distillation for IFNet

Directly approximating the intermediate flows is challenging because of no access to the intermediate frame and the lack of supervision. To address this problem, we design a privileged distillation loss to our IFNet. We stack an additional IFBlock (teacher model) that refines the results IFNet refers to the ground truth (privileged information). The dis-

tillation loss  $\mathcal{L}_{dis}$  is defined as follows:

$$\mathcal{L}_{dis} = \sum_{i \in \{0,1\}} \|F_{t \rightarrow i} - F_{t \rightarrow i}^{Tea}\|_1. \quad (4)$$

We apply the distillation loss over the full sequence of predictions generated from the iteratively updating process in our student model. The gradient of this loss will not be back-propagated to the teacher model. With the access of the target frame  $I_t^{GT}$  as privileged information, our teacher model has a different view of the video clip with the student. In the experiments section, we show that this supervision is beneficial to the training of our whole system.

### Implement Details

**Supervisions.** Given a pair of consecutive frames,  $I_0, I_1$ , our training loss  $\mathcal{L}$  is a linear combination of the reconstruction loss and privileged distillation loss  $\mathcal{L}_{dis}$ :

$$\mathcal{L} = \mathcal{L}_{rec} + \mathcal{L}_{rec}^{Tea} + \lambda_d \mathcal{L}_{dis}, \quad (5)$$

where we set  $\lambda_d = 0.01$  to balance the scale of losses.

The reconstruction loss  $\mathcal{L}_{rec}$  models the reconstruction quality of the intermediate frame. We denote the synthesized frame by  $\hat{\mathbf{I}}_t$  and the ground-truth frame by  $\mathbf{I}_t^{GT}$ . The reconstruction loss has the formulation of:

$$\mathcal{L}_{rec} = d(\hat{\mathbf{I}}_t - \mathbf{I}_t^{GT}), \mathcal{L}_{rec}^{Tea} = d(\hat{\mathbf{I}}_t^{Tea}, \mathbf{I}_t^{GT}). \quad (6)$$

where  $d$  is usually pixel-wised  $L_1$  loss. Following previous work (Niklaus and Liu 2018, 2020), we experimentally confirm that replacing the original  $L_1$  loss with the  $L_1$  loss between two Laplacian pyramid representations of the reconstructed image and ground truth (denoted as  $L_{Lap}$ ) can produce slightly better quantitative results.

**Training dataset.** We use the Vimeo90K dataset (Xue et al. 2019) to train our model. This dataset has 51,312 triplets for training, where each triplet contains three consecutive video frames with a resolution of  $256 \times 448$ . We randomly augment the training data by horizontal and vertical flipping and temporal order reversing.

**Training strategy.** We train RIFE from scratch on the Vimeo90K training set to predict the middle frame given the frames on both sides. RIFE is optimized by AdamW (Loshchilov and Hutter 2017) with weight decay  $10^{-4}$  for 300 epochs with  $224 \times 224$  patches on the Vimeo90K training set. Our training uses a batch size of 64. We gradually reduce the learning rate from  $3 \times 10^{-4}$  to  $3 \times 10^{-5}$  using cosine annealing during the whole training process. We train RIFE on four NVIDIA TITAN X (Pascal) GPUs for about 15 hours.

### Experiments

We first introduce the benchmarks for evaluation. Then we provide variants of our models with different computational costs. We compare these models with representative state-of-the-art methods, both quantitatively and visually. An ablation study is carried out to analyze our design. In addition, we show the capability of generating multiple frames using our models. Finally, we discuss some limitations of RIFE.

Table 2: **Quantitative comparisons on the UCF101 (Soomro, Zamir, and Shah 2012), Vimeo90K (Xue et al. 2019), Middlebury-OTHER set (Baker et al. 2011), and HD benchmarks (Bao et al. 2018).** To evaluate models using quantitative metrics, the images of each dataset are directly inputted. Some models are unable to run on 1080p images due to exceeding the memory available on our graphics card (denoted as “OOM”). To report the runtime, we test all models for processing a pair of  $640 \times 480$  images. The numbers in **red** and **blue** represent the best and second-best performance. We use gray backgrounds to mark the methods that require pre-trained models to approximate the image depth, contextual map or optical flow.

Method	# Parameters (Million)	Runtime (ms)	UCF101		Vimeo90K		M.B.	HD
			PSNR	SSIM	PSNR	SSIM	IE	PSNR
DVF† (ICCV’17)	<u>1.6</u>	80	34.12	0.963	31.54	0.946	4.04	-
PWC-Net† (CVPR’18)	8.8	54	33.60	0.963	31.36	0.939	2.24	-
SuperSlomo† (CVPR’18)	19.8	52	34.75	0.968	33.15	0.966	2.28	-
SepConv (ICCV’17)	21.6	51	34.78	0.967	33.79	0.970	2.27	30.87
TOFlow (IJCV’19)	<b>1.1</b>	84	34.58	0.967	33.73	0.968	2.15	29.37
MEMC-Net (TPAMI’19)	70.3	120‡(401)	35.01	0.968	34.29	0.970	2.12	31.39
DAIN (CVPR’19)	24.0	130‡(436)	35.00	0.968	34.71	0.976	2.04	31.64‡(OOM)
DSepConv (AAAI’20)	21.8	236	35.08	0.969	34.73	0.974	2.03	OOM
CAIN (AAAI’20)	42.8	38	34.98	0.969	34.65	0.973	2.28	31.77
SoftSplat (CVPR’20)	7.7	135	<b>35.39</b>	<b>0.970</b>	<b>36.10</b>	<b>0.980</b>	<b>1.81</b>	-
AdaCoF (CVPR’20)	21.8	<b>34</b>	34.91	0.968	34.27	0.971	2.31	31.43
BMBC (ECCV’20)	11.0	1580	35.15	0.969	35.01	0.976	2.04	OOM
CDFI (CVPR’21)	5.0	198	35.21	0.969	35.17	0.977	1.98	OOM
EDSC (ArXiv’21)	8.9	46	35.13	0.968	34.84	0.975	2.02	31.59
DVF (Trained on Vimeo90K)	<u>1.6</u>	80	34.92	0.968	34.56	0.973	2.47	31.47
RIFE	9.8	<b>16</b>	35.28	0.969	35.62	0.978	1.96	<b>32.14</b>
RIFE-Large (2T2R)	9.8	80	<b>35.41</b>	<b>0.970</b>	<b>36.12</b>	<b>0.980</b>	<b>1.92</b>	<b>32.32</b>

‡: are not trained with Vimeo90K (Xue et al. 2019) training dataset.

‡: copy from (Bao et al. 2019), we compile released models and get three times slower on our graphics card.

## Benchmarks and Evaluation Metrics

We train our models on the Vimeo90K training dataset and directly test it on the following benchmarks.

**Middlebury.** The Middlebury (M.B.) benchmark (Baker et al. 2011) is widely used to evaluate VFI methods. The image resolution in this dataset is around  $640 \times 480$ . We report the average IE of the Middlebury-OTHER set.

**Vimeo90K.** There are 3,782 triplets in the Vimeo90K testing set (Xue et al. 2019) with resolution of  $448 \times 256$ .

**UCF101.** The UCF101 dataset (Soomro, Zamir, and Shah 2012) contains videos with a large variety of human actions. There are 379 triplets with a resolution of  $256 \times 256$ .

**HD.** Bao *et al.* (Bao et al. 2018) collect 11 high-resolution videos for evaluation. The HD benchmark consists of four 1080p, three 720p and four  $1280 \times 544$  videos. Following the author of this benchmark, we use the first 100 frames of each video for evaluation.

We measure the peak signal-to-noise ratio (PSNR), structural similarity (SSIM), and interpolation error (IE) for quantitative evaluation. All the methods are tested on a TITAN X (Pascal) GPU. We calculate the average process time for 100 runs after a warm-up process of 100 runs.

## Test-Time Augmentation and Model Scaling

We provide some models with different computation overheads and performance to meet different needs by model scaling. We introduce two methods following: test-time aug-

Table 3: **Increase model complexity to achieve better quantitative results.**  $2T$  represents inferring additional one result by flipping the inputs, and the final results are the average of the two results.  $2R$  represents removing the first downsampling layer of IFNet and the first one of RefineNet.

Model Setting	RIFE	$2T$	$2R$	$2T2R$
UCF101 PSNR	35.28	35.35	35.34	<b>35.41</b>
Vimeo90K PSNR	35.61	35.76	35.98	<b>36.12</b>
M.B. IE	1.96	1.93	1.94	<b>1.92</b>
HD PSNR	32.14	32.26	32.16	<b>32.32</b>
# Parameters	9.8M	9.8M	9.8M	9.8M
Runtime*	<b>35ms</b>	67ms	126ms	240ms
Complexity*	<b>200G</b>	400G	790G	1580G

\*: on 720p frames ( $batchsize = 1$ )

mentation and resolution multiplying. We flip the input images horizontally and vertically to get augmented test data. Then we use the same model to infer some results and reverse the flipping. When the two results are averaged, the relative benefit is the largest (denoted as RIFE- $2T$ ). Moreover, we remove a downsample layer from the headers of IFNet and RefineNet upon RIFE base model, which doubles the feature map’s resolution that produces a model named RIFE- $2R$ . We can combine these two modifications to produce a model named RIFE-Large ( $2T2R$ ). The performance and runtime for these models is reported in Table 3 and de-

picted in Figure 1. Furthermore, we show that simply increasing model capacity can effectively improve model performance.

## Comparisons with Previous Methods

We compare RIFE with previous VFI models including DVF (Liu et al. 2017), SuperSlomo (Jiang et al. 2018), TOFlow (Xue et al. 2019), SepConv (Niklaus, Mai, and Liu 2017b), MEMC-Net (Bao et al. 2018), DAIN (Bao et al. 2019), CAIN (Choi et al. 2020), SoftSplat (Niklaus and Liu 2020), BMBC (Park et al. 2020), DSepConv (Cheng and Chen 2020b), AdaCoF (Lee et al. 2020a), CDFI (Ding et al. 2021) and EDSC (Cheng and Chen 2020a). For PWC-Net (Sun et al. 2018), we use an occlusion reasoning algorithm (Baker et al. 2011) to interpolate intermediate frame (Choi et al. 2020). These models are officially released except SoftSplat. SoftSplat is not fully open-sourced and its results are reported by the origin authors. In addition, we train a DVF model using Vimeo90K dataset to show the potential of directly estimating intermediate flows using CNNs. We report the performance in Table 2.

RIFE runs considerably faster than other methods. Meanwhile, RIFE needs only 3.1 gigabytes of GPU memory to process 1080p videos, while some methods exceed 12 gigabytes. When using RIFE to process video frames in parallel ( $batchsize = 4$ ), the total runtime can further drop to half. We get a larger version of our model (RIFE-Large) by model scaling and test-time augmentation, which runs about 1.7 times faster than the previous state-of-the-art method SoftSplat (Niklaus and Liu 2020) with comparable performance. Compared with SoftSplat, RIFE does not require a specially designed forward warping operator or any pre-trained optical flow model. We provide a visual comparison of video clips with large motions from the Vimeo90K testing set in Figure 5, where SepConv (Niklaus, Mai, and Liu 2017b) and DAIN (Bao et al. 2019) produce ghosting artifacts, and CAIN (Choi et al. 2020) causes missing-parts artifacts. Overall, our method can produce more reliable results.

## Ablation Study

We design an ablation study on the distillation scheme, intermediate flow estimation, and model design, shown in Table 4. These experiments use the same hyper-parameter setting and evaluation on Vimeo90K (Xue et al. 2019) and MiddleBury (Baker et al. 2011) benchmarks.

**Ablation on the distillation scheme.** To analyze the contributions of privileged distillation loss  $\mathcal{L}_{dis}$ , we design several experiments. We notice removing the distillation scheme will make the model’s training unstable and result in a much worse result. Further, we implement another two distillation methods. Firstly, we remove the privileged teacher block and use the last IFBlock’s results to guide the first two IFBlocks, denoted as “self-consistency”. Secondly, we use a pre-trained state-of-the-art optical flow model, RAFT (Teed and Deng 2020), as the privileged teacher model to estimate the intermediate flows based on the ground truth image. This guidance is inspired by the pseudo-labels method (Lee et al.

Table 4: Ablation study on distillation scheme, intermediate flow estimation, model design and losses.

Setting	Vimeo90K PSNR	M.B. IE	Runtime ms(720p)
RIFE w/o distillation	35.22	2.15	34
RIFE w/ self-consistency	35.38	2.02	34
RIFE w/ RAFT-KD	<u>35.42</u>	<u>1.99</u>	34
RIFE	<b>35.61</b>	<b>1.96</b>	34
RAFT + linear combination	34.68	2.31	<u>168</u>
RAFT + CNN reversal	34.82	2.24	181
RAFT + reversal layer	35.16	<u>2.04</u>	282
PWC-Net + reversal layer	<u>35.24</u>	2.06	232
RIFE	<b>35.61</b>	<b>1.96</b>	<b>34</b>
RIFE w/o RefineNet	34.82	2.21	<b>17</b>
RIFE w/ 1 IFBlock	35.22	2.13	<u>23</u>
RIFE w/ 2 IFBlocks	<u>35.49</u>	<u>1.98</u>	29
RIFE	<b>35.61</b>	<b>1.96</b>	34
RIFE w/ $L_1$	<u>35.46</u>	<b>1.94</b>	34
RIFE w/ $L_{Lap}$	<b>35.61</b>	<u>1.96</u>	34

2013), denoted as “RAFT-KD”. However, this implementation relies on the pre-trained optical model and extremely increases the training duration. These experiments argue the importance of optical flow supervision, and the privileged distillation scheme for RIFE is the most effective.

**IFNet vs. flow reversal.** To demonstrate the effectiveness of IFNet, we compare it with previous intermediate flow estimation methods. Specifically, we use RAFT (Teed and Deng 2020) and PWC-Net (Sun et al. 2018) with officially pre-trained parameters to estimate the bi-directional flows. Then we implement three flow reversal methods, including linear combination (Jiang et al. 2018), using a hidden convolutional layer with 128 channels, and the flow reversal method from EQVI (Liu et al. 2020) consisting of a reversal layer and a U-Net filter. The optical flow models and flow reversal modules are combined together to replace the IFNet. They are jointly trained with RefineNet. Because these models can not directly approximate the fusion map, the fusion map is subsequently approximated by RefineNet. As shown in Table 4, RIFE is more efficient and gets better interpolation performance. These flow models can estimate accurate bi-directional optical flow, but the flow reversal has difficulties in dealing with object position changes. We argue that the current optical flow reversals are not effective and efficient enough.

**Ablation on RIFE’s architecture.** To study the model design, we remove the RefineNet and residual term, resulting in blurry results and performance degradation as in Table 4. To verify the coarse-to-fine strategy of IFNet, we removed the first IFBlock and the first two IFBlocks in two experiments, respectively. These experiments confirm the effectiveness of RIFE model.

**Ablation on losses.** We provide a pair of experiments to show  $L_{Lap}$  is slightly better than  $L_1$ .

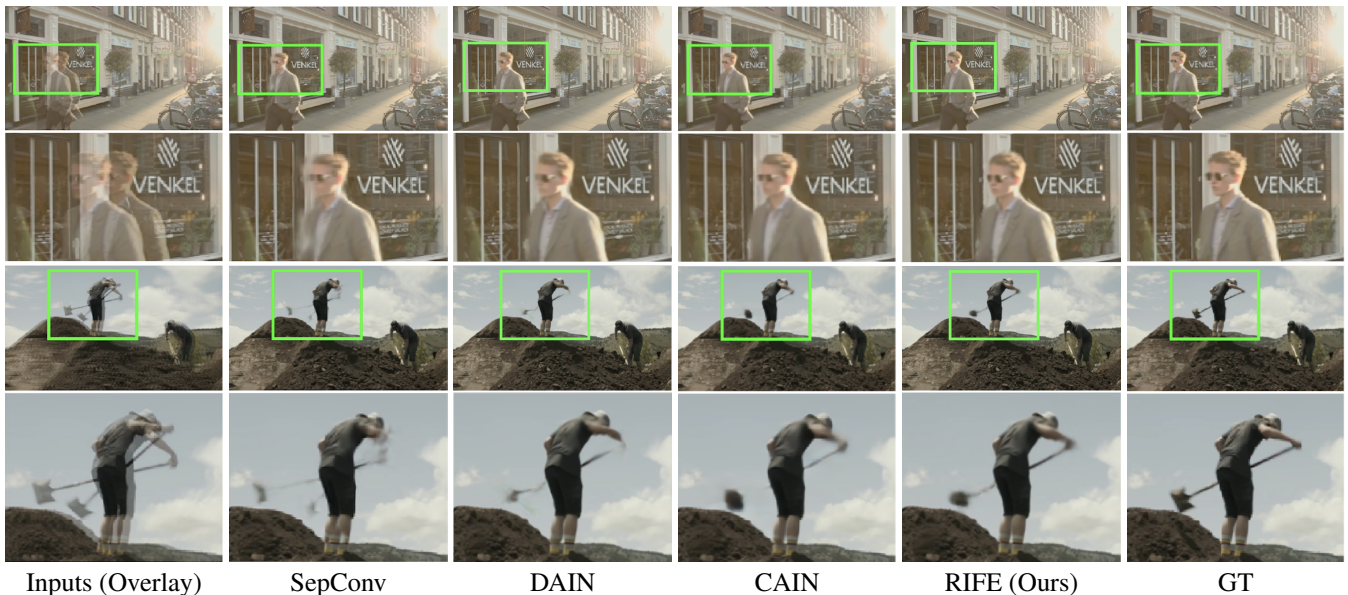


Figure 5: **Qualitative comparison on Vimeo90K (Xue et al. 2019) testing set.** We cut out the objects and zoom in them (Choi et al. 2020). While other methods cause various artifacts, our method produces good effects on the moving objects.

Table 5: **Quantitative evaluation for  $8\times$  interpolation on the HD benchmark (Bao et al. 2018).**

Method	Recursion	$544 \times 1280$	720p	1080p
DAIN	✓	<b>19.32</b>	<b>28.81</b>	OOM
DAIN	-	<u>19.03</u>	27.97	OOM
CAIN	✓	18.37	28.31	24.71
BMBC	✓	18.16	26.70	OOM
BMBC	-	17.12	19.60	OOM
DSepconv	✓	16.80	19.57	OOM
CDFI	✓	18.72	26.91	OOM
EDSC <sub>s</sub>	✓	18.15	28.39	24.22
EDSC <sub>m</sub> †	-	18.89	27.03	<b>25.49</b>
RIFE	✓	<u>19.03</u>	<b>29.14</b>	<u>24.87</u>

†: use additional multiple frame training dataset.

## Generating Multiple Frames

We can apply RIFE recursively to interpolate multiple intermediate frames at different timesteps  $t \in (0, 1)$ . Specifically, given two consecutive input frames  $I_0, I_1$ , we apply RIFE once to get intermediate frame  $\hat{I}_{0.5}$  at  $t = 0.5$ . We feed  $I_0$  and  $\hat{I}_{0.5}$  to get  $\hat{I}_{0.25}$ , and we can repeat this process recursively to interpolate multiple frames. We provide the visual results for  $8\times$  settings in the Appendix.

Although recursive method can reconstruct the multi-frame results, the error may be accumulated. To provide a quantitative comparison for  $8\times$  interpolation, we further extract  $8k^{th}$  ( $0 \leq 8k < 100$ ) of every video from HD benchmark (Bao et al. 2018) and use them to interpolate other frames. We divide the HD benchmark into three subsets with different resolution frames to test these methods. We show the quantitative PSNR between generated frames and frames of the origin videos in Table 5. Note that DAIN (Bao et al.

2019), BMBC (Park et al. 2020) and EDSC<sub>m</sub> (Cheng and Chen 2020b) can generate a frame at an arbitrary time between the input ones. But they do not show obvious improvement over recursive VFI methods. Although some non-recursive methods (Jiang et al. 2018; Bao et al. 2019) do not need to repeatedly estimate the optical flows, the occlusion approximation, flow reversal and eliminating artifacts for each target frame still need additional calculation. Overall, RIFE is still practical in the  $8\times$  interpolation scenario.

## Limitations

Our work may not cover some real application requirements. First, RIFE does not support directly generating frames at an arbitrary timestep. This defect is common to most VFI methods. The models with flow reversal components may be suitable for this scene (Jiang et al. 2018; Bao et al. 2019). Second, RIFE focuses on only using two input frames while multi-frame input is argued to be useful (Xu et al. 2019; Liu et al. 2020; Kalluri et al. 2020). Third, many previous VFI papers point out that SSIM and PSNR are not consistent with human perception (Niklaus, Mai, and Liu 2017a; Niklaus and Liu 2020). Because distortion and perceptual quality are at odds with each other (Blau and Michaeli 2018), we focus on improving the distortion quality.

## Conclusion

In this work, we analyze and compare the recent flow-based VFI methods. We further develop an efficient and flexible algorithm for VFI, named RIFE. With the more accurate intermediate flow estimation, RIFE can effectively process videos of different resolution and interpolate multiple frames between input frames. The state-of-the-art results of RIFE shed light for future research on flow-based interpolation methods.

## References

- Anil, R.; Pereyra, G.; Passos, A.; Ormandi, R.; Dahl, G. E.; and Hinton, G. E. 2018. Large scale distributed neural network training through online distillation. *arXiv preprint arXiv:1804.03235*.
- Baker, S.; Scharstein, D.; Lewis, J.; Roth, S.; Black, M. J.; and Szeliski, R. 2011. A database and evaluation methodology for optical flow. In *International Journal of Computer Vision (IJCV)*.
- Bao, W.; Lai, W.-S.; Ma, C.; Zhang, X.; Gao, Z.; and Yang, M.-H. 2019. Depth-aware video frame interpolation. In *Proceedings of the IEEE Conference on Computer Vision and Pattern Recognition (CVPR)*.
- Bao, W.; Lai, W.-S.; Zhang, X.; Gao, Z.; and Yang, M.-H. 2018. MEMC-Net: Motion Estimation and Motion Compensation Driven Neural Network for Video Interpolation and Enhancement. *IEEE Transactions on Pattern Analysis and Machine Intelligence (IEEE TPAMI)*.
- Blau, Y.; and Michaeli, T. 2018. The perception-distortion tradeoff. In *Proceedings of the IEEE Conference on Computer Vision and Pattern Recognition (CVPR)*.
- Chen, X.; Zhang, Y.; Wang, Y.; Shu, H.; Xu, C.; and Xu, C. 2020. Optical flow distillation: Towards efficient and stable video style transfer. In *Proceedings of the European Conference on Computer Vision (ECCV)*.
- Cheng, X.; and Chen, Z. 2020a. Multiple video frame interpolation via enhanced deformable separable convolution. *arXiv preprint arXiv:2006.08070*.
- Cheng, X.; and Chen, Z. 2020b. Video frame interpolation via deformable separable convolution. In *Proceedings of the Association for the Advancement of Artificial Intelligence (AAAI)*.
- Choi, M.; Kim, H.; Han, B.; Xu, N.; and Lee, K. M. 2020. Channel Attention Is All You Need for Video Frame Interpolation. In *Proceedings of the Association for the Advancement of Artificial Intelligence (AAAI)*.
- Ding, T.; Liang, L.; Zhu, Z.; and Zharkov, I. 2021. CDFI: Compression-Driven Network Design for Frame Interpolation. In *Proceedings of the IEEE Conference on Computer Vision and Pattern Recognition (CVPR)*.
- Dosovitskiy, A.; Fischer, P.; Ilg, E.; Hausser, P.; Hazirbas, C.; Golkov, V.; Van Der Smagt, P.; Cremers, D.; and Brox, T. 2015. FlowNet: Learning optical flow with convolutional networks. In *Proceedings of the IEEE International Conference on Computer Vision (ICCV)*.
- He, K.; Zhang, X.; Ren, S.; and Sun, J. 2015. Delving deep into rectifiers: Surpassing human-level performance on imagenet classification. In *Proceedings of the IEEE International Conference on Computer Vision (ICCV)*.
- Hinton, G.; Vinyals, O.; and Dean, J. 2015. Distilling the knowledge in a neural network. *arXiv preprint arXiv:1503.02531*.
- Hui, T.-W.; Tang, X.; and Change Loy, C. 2018. Liteflownet: A lightweight convolutional neural network for optical flow estimation. In *Proceedings of the IEEE Conference on Computer Vision and Pattern Recognition (CVPR)*.
- Ilg, E.; Mayer, N.; Saikia, T.; Keuper, M.; Dosovitskiy, A.; and Brox, T. 2017. FlowNet 2.0: Evolution of optical flow estimation with deep networks. In *Proceedings of the IEEE Conference on Computer Vision and Pattern Recognition (CVPR)*.
- Jiang, H.; Sun, D.; Jampani, V.; Yang, M.-H.; Learned-Miller, E.; and Kautz, J. 2018. Super sloMo: High quality estimation of multiple intermediate frames for video interpolation. In *Proceedings of the IEEE Conference on Computer Vision and Pattern Recognition (CVPR)*.
- Jonschkowski, R.; Stone, A.; Barron, J. T.; Gordon, A.; Konolige, K.; and Angelova, A. 2020. What Matters in Unsupervised Optical Flow. In *Proceedings of the European Conference on Computer Vision (ECCV)*.
- Kalluri, T.; Pathak, D.; Chandraker, M.; and Tran, D. 2020. FLAVR: Flow-Agnostic Video Representations for Fast Frame Interpolation. *arXiv preprint arXiv:2012.08512*.
- Lee, D.-H.; et al. 2013. Pseudo-label: The simple and efficient semi-supervised learning method for deep neural networks. In *Proceedings of the IEEE International Conference on Machine Learning Workshop (ICMLW)*.
- Lee, H.; Kim, T.; Chung, T.-y.; Pak, D.; Ban, Y.; and Lee, S. 2020a. Adacof: Adaptive collaboration of flows for video frame interpolation. In *Proceedings of the IEEE Conference on Computer Vision and Pattern Recognition (CVPR)*.
- Lee, W.; Lee, J.; Kim, D.; and Ham, B. 2020b. Learning with privileged information for efficient image super-resolution. In *Proceedings of the European Conference on Computer Vision (ECCV)*.
- Liu, Y.; Xie, L.; Siyao, L.; Sun, W.; Qiao, Y.; and Dong, C. 2020. Enhanced quadratic video interpolation. In *Proceedings of the European Conference on Computer Vision (ECCV)*.
- Liu, Z.; Yeh, R. A.; Tang, X.; Liu, Y.; and Agarwala, A. 2017. Video frame synthesis using deep voxel flow. In *Proceedings of the IEEE International Conference on Computer Vision (ICCV)*.
- Lopez-Paz, D.; Bottou, L.; Schölkopf, B.; and Vapnik, V. 2015. Unifying distillation and privileged information. *arXiv preprint arXiv:1511.03643*.
- Loshchilov, I.; and Hutter, F. 2017. Fixing Weight Decay Regularization in Adam. *arXiv preprint arXiv:1711.05101*.
- Luo, K.; Wang, C.; Liu, S.; Fan, H.; Wang, J.; and Sun, J. 2021. UPFlow: Upsampling Pyramid for Unsupervised Optical Flow Learning.
- Meister, S.; Hur, J.; and Roth, S. 2018. UnFlow: Unsupervised Learning of Optical Flow with a Bidirectional Census Loss. In *Proceedings of the Association for the Advancement of Artificial Intelligence (AAAI)*.
- Meyer, S.; Wang, O.; Zimmer, H.; Grosse, M.; and Sorkine-Hornung, A. 2015. Phase-based frame interpolation for video. In *Proceedings of the IEEE Conference on Computer Vision and Pattern Recognition (CVPR)*.
- Niklaus, S.; and Liu, F. 2018. Context-aware synthesis for video frame interpolation. In *Proceedings of the IEEE Conference on Computer Vision and Pattern Recognition (CVPR)*.



Niklaus, S.; and Liu, F. 2020. Softmax Splatting for Video Frame Interpolation. In *Proceedings of the IEEE Conference on Computer Vision and Pattern Recognition (CVPR)*.

Niklaus, S.; Mai, L.; and Liu, F. 2017a. Video frame interpolation via adaptive convolution. In *Proceedings of the IEEE Conference on Computer Vision and Pattern Recognition (CVPR)*.

Niklaus, S.; Mai, L.; and Liu, F. 2017b. Video frame interpolation via adaptive separable convolution. In *Proceedings of the IEEE International Conference on Computer Vision (ICCV)*.

Park, J.; Ko, K.; Lee, C.; and Kim, C.-S. 2020. BMBC: Bilateral Motion Estimation with Bilateral Cost Volume for Video Interpolation. In *Proceedings of the European Conference on Computer Vision (ECCV)*.

Porrello, A.; Bergamini, L.; and Calderara, S. 2020. Robust re-identification by multiple views knowledge distillation. In *Proceedings of the European Conference on Computer Vision (ECCV)*.

Reda, F. A.; Sun, D.; Dundar, A.; Shoeybi, M.; Liu, G.; Shih, K. J.; Tao, A.; Kautz, J.; and Catanzaro, B. 2019. Unsupervised video interpolation using cycle consistency. In *Proceedings of the IEEE International Conference on Computer Vision (ICCV)*.

Ronneberger, O.; Fischer, P.; and Brox, T. 2015. U-net: Convolutional networks for biomedical image segmentation. In *International Conference on Medical image computing and computer-assisted intervention (MICCAI)*.

Soomro, K.; Zamir, A. R.; and Shah, M. 2012. UCF101: A Dataset of 101 Human Actions Classes From Videos in The Wild. *CoRR*, abs/1212.0402.

Sun, D.; Yang, X.; Liu, M.-Y.; and Kautz, J. 2018. Pwc-net: Cnns for optical flow using pyramid, warping, and cost volume. In *Proceedings of the IEEE Conference on Computer Vision and Pattern Recognition (CVPR)*.

Teed, Z.; and Deng, J. 2020. RAFT: Recurrent All-Pairs Field Transforms for Optical Flow. In *Proceedings of the European Conference on Computer Vision (ECCV)*.

Wu, C.-Y.; Singhal, N.; and Krahenbuhl, P. 2018. Video compression through image interpolation. In *Proceedings of the European Conference on Computer Vision (ECCV)*.

Xu, X.; Siyao, L.; Sun, W.; Yin, Q.; and Yang, M.-H. 2019. Quadratic video interpolation. In *Advances in Neural Information Processing Systems (NIPS)*.

Xue, T.; Chen, B.; Wu, J.; Wei, D.; and Freeman, W. T. 2019. Video enhancement with task-oriented flow. In *International Journal of Computer Vision (IJCV)*.

Yuan, S.; Stenger, B.; and Kim, T.-K. 2019. RGB-based 3D hand pose estimation via privileged learning with depth images. In *Proceedings of the IEEE International Conference on Computer Vision Workshop (ICCVW)*.

## Appendix

### Architecture of RefineNet

Following the previous work (Niklaus and Liu 2020), we design a RefineNet with an encoder-decoder architecture similar to U-Net and a context extractor. The context extractor and encoder part have similar architectures, consisting of four convolutional blocks, and each of them is composed of two  $3 \times 3$  convolutional layers, respectively. The decoder part in the FusionNet has four transpose convolution layers. We use sigmoid function to restrict the outputs of RefineNet.

Specifically, the context extractor first extracts the pyramid contextual features from input frames separately. We denote the pyramid contextual feature as  $C_0: \{C_0^0, C_0^1, C_0^2, C_0^3\}$  and  $C_1: \{C_1^0, C_1^1, C_1^2, C_1^3\}$ . We then perform backward warping on these features using estimated intermediate flows to produce aligned pyramid features,  $C_{t \leftarrow 0}$  and  $C_{t \leftarrow 1}$ . The origin frames  $I_0, I_1$ , warped frames  $\hat{I}_{t \leftarrow 0}, \hat{I}_{t \leftarrow 1}$ , intermediate flows  $F_{t \rightarrow 0}, F_{t \rightarrow 1}$  and fusion mask  $M$  are fed into the encoder. The output of  $i$ -th encoder block is concatenated with the  $C_{t \leftarrow 0}^i$  and  $C_{t \leftarrow 1}^i$  before being fed into the next block. The decoder parts finally produce a reconstruction residual  $\Delta$ . And we will get a refined reconstructed image  $clamp(\hat{I}_t + \Delta, 0, 1)$ , where  $\hat{I}_t$  is the reconstruct image before the Refine Net. We show some visualization results in Figure 8. RefineNet seems to make some uncertain areas more blurred to improve quantitative results. For this inconsistency of distortion and perceptual quality, please refer to “the Perception-Distortion tradeoff” (Blau and Michaeli 2018).

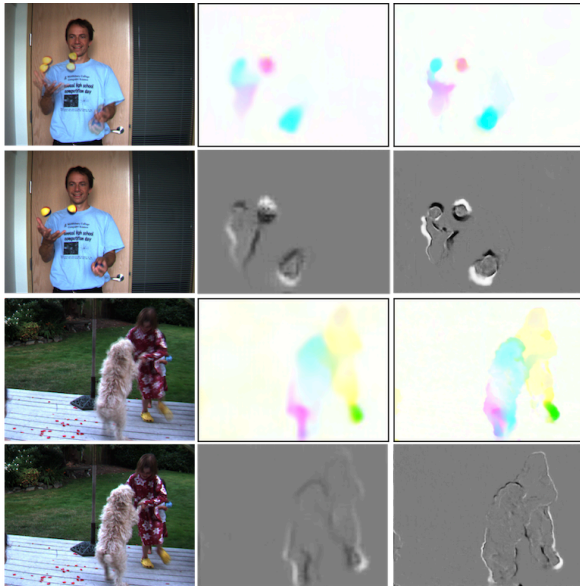


Figure 6: **Visualization of intermediate flow  $F_{t \rightarrow 0}$  and blend mask  $M$ .** We show that stack 3 IFblocks can get finer intermediate flow and blend mask.

### Training Dynamic

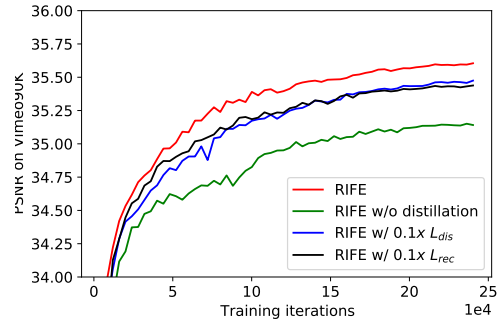


Figure 7: **PSNR on Vimeo90K benchmark during the whole training process.** The distillation scheme helps RIFE converge to better performance

We study the dynamic during the RIFE training. As shown in Figure 7, the privileged distillation scheme helps RIFE converge to better performance. Furthermore, we try to adjust the weights of losses. We found that larger scale ( $10 \times$ ) of weights will cause the model to not converge and smaller weights ( $0.1 \times$ ) will slightly reduce model performance.

### Multiframe Interpolation

We select several images with large motions from the Vimeo90K benchmark in Figure 9. We observe that RIFE successfully produces smooth and continuous motions.

### Model Efficiency Comparison

The speed of models is very important in frame interpolation applications. However, to the best of our knowledge, currently published papers do not test the speed of each state-of-the-art VFI model on same hardware, and rarely report the complexity of the model. Some previous works report runtime data from the MiddleBury public leaderboard without indicating running devices. These data are reported by the submitters of various methods. A more reliable survey comes from EDSC (Table 10) (Cheng and Chen 2020a). We collect the models of each paper and test them on a NVIDIA TITAN X(Pascal) GPU with same environment.

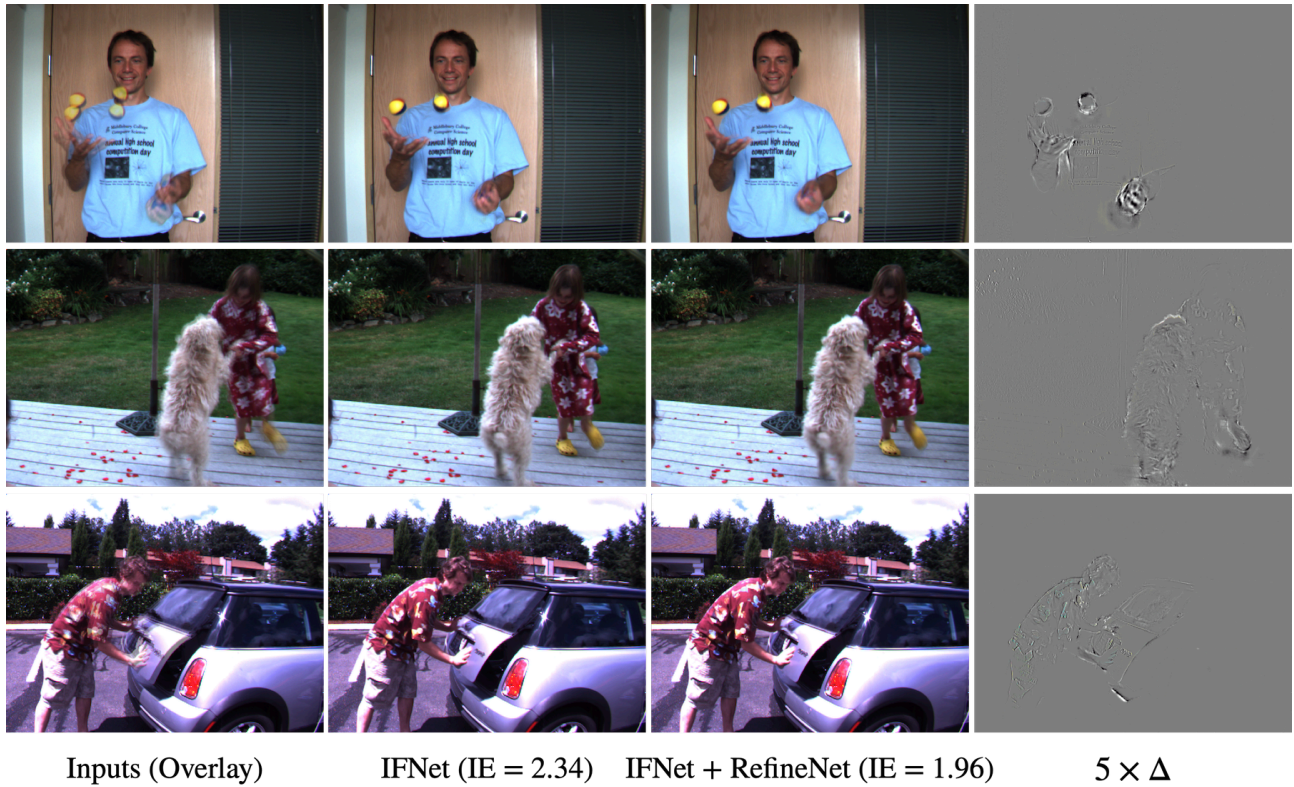


Figure 8: **Interpolating results on the Middlebury (Baker et al. 2011) dataset.** We show that the function of RefineNet is mainly to refine the high frequency content of the results.

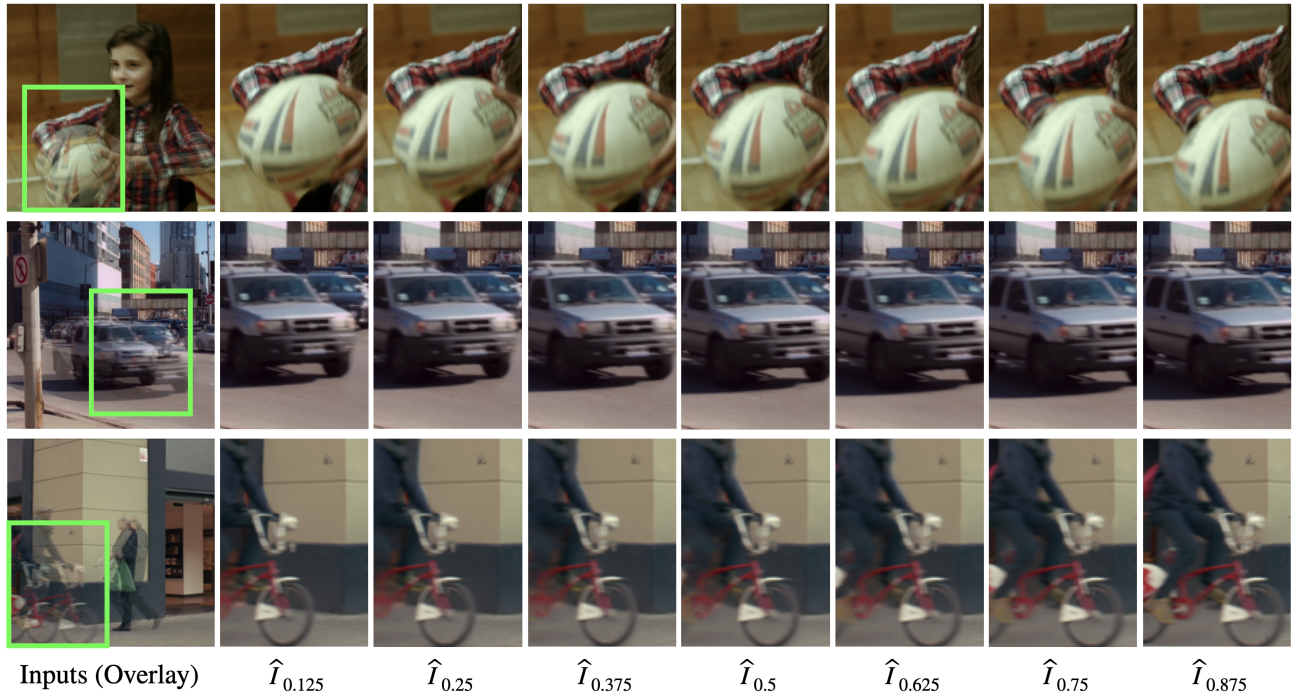


Figure 9: **Interpolating multiple frames on the Vimeo90K testing dataset by applying RIFE recursively.** We cut out the moving objects according to the green boxes and zoom in the results. RIFE provides smooth and continuous motions.